Experimental Progress in Simultaneous Ionization-Excitation Processes

Mark Stevenson, Mevlut Dogan[1] and Albert Crowe

School of Natural Sciences (Physics), University of Newcastle upon Tyne, NE1 7RU, United Kingdom
[1]Present address: Kocatepe University, Afyon, Turkey

Abstract. A number of experimental techniques are now being used in different laboratories to study electron impact simultaneous ionization-excitation in atoms. Here experimental studies, mostly from this laboratory, using the (e,eγ) and (e,2e) techniques are discussed. Data are presented for the He^+ (n = 2, 3, 4) states and the Ca^+ (4p) $^2P_{3/2}$ state.

INTRODUCTION

It is now three decades since the first complete electron impact excitation experiment [1] was reported. Data from this and subsequent (e,eγ) experiments have provided a severe test of theoretical models and it is only within the last decade, with the introduction of the Convergent Close Coupling [2] and R-matrix with pseudo-states [3] methods, that a detailed description of the experimental data has been realized over a wide range of kinematics, even for simple targets like helium. On the other hand, the overwhelming majority of electron impact correlation studies of ionization have been of the (e,2e) type [4]. Although these are kinematically complete, they yield cross sections which give only the magnitude of scattering amplitudes but no phase information.

The production of ions in excited states presents new experimental and theoretical challenges. They provide the opportunity for complete ionization experiments [5], but only by conducting a triple coincidence (e,2eγ) experiment. Theoretically, ionization-excitation is a highly correlated process with both the incident and two atomic electrons changing state during the collision. However, in parallel with increasing experimental effort, realistic theoretical models are now being developed [6].

Helium is the simplest two-electron system and electron-photon angular correlation data, as well as double differential cross sections (DDCS) from electron-photon coincidence studies, are presented for the He^+(2p)state. (e,2e) data are also given for the individual He^+(n = 2, 3, 4) states.

Using our techniques, the low cross section for He^+(2p) production and the short wavelength (30.4 nm) of the photon emitted in its decay to the ground state ion makes this an unattractive process for a complete (e,2eγ) experiment [7]. These experimental difficulties are overcome by studying heavier systems. We have chosen calcium as an ideal experimental target [8] and one which will also present a realistic challenge for theory [9]. First experimental results from this target are discussed.

CP697, *Correlation and Polarization in Photonic, Electronic, and Atomic Collisions,* edited by G. F. Hanne et al.

The experimental set-up for helium has been discussed previously [10, 11] and the same apparatus has been used for the calcium studies with a calcium oven replacing the helium source.

HELIUM

The process,

$$\begin{array}{l} e + \mathrm{He}\ (1s^2)\ ^1S \rightarrow \mathrm{He}^+\ (2p)\ ^2P + e\ (\text{scattered}) + e\ (\text{ejected}) \\ \qquad\qquad\qquad\qquad \downarrow \\ \qquad\qquad\qquad\quad \mathrm{He}^+\ (1s)\ ^2S + h\nu\ (30.4\ \text{nm}), \end{array}$$

has been studied using the (e,eγ) and (e,2e) techniques.

(e,eγ) Studies

Typical DDCS are shown in figure 1, determined from the coincidence signal between the 30.4 nm photon and the fast scattered electron, as a function of its energy [10,12,13]. The data show the generally accepted DDCS shape for ionization processes, peaking at the maximum scattered electron energy and falling off as the energy decreases. However, from the structure in the DDCS it is clear that indirect processes are contributing to the observed signal. The structure corresponding to an ejected electron energy of 4.3 eV arises from autoionization of doubly excited 3*l*3*l'* states. Further structure is observed corresponding to higher ejected electron energies,

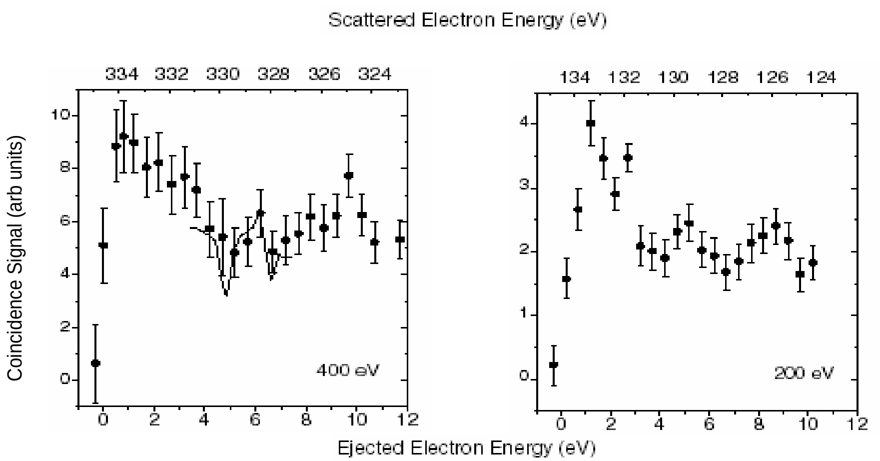

FIGURE 1. DDCS for He^+ (2p) as a function of the detected electron energy (top scale) for incident electron energies of 200 eV and 400 eV. The bottom scale shows the energy of the undetected electron. At 400 eV the solid line in the resonance region is a calculation due to Balashov [14].

but at these energies the technique cannot distinguish between autoionization from higher lying states and cascade from the $He^+(n \geq 3)$ states.

Angular correlations between scattered electrons and the 30.4 nm photons have been measured for a range of scattered electron energies and angles. The measured correlations can be expressed in the form [10],

$$I(\theta) \sim 1 - A \cos 2(\theta - \gamma).$$

Figure 2 shows the amplitude A and alignment angle γ for an incident electron energy of 200 eV and a detected electron energy of 133.4 eV. Excellent agreement is obtained between experiment and theory for the γ parameter but there is a lack of agreement between the two experiments and with the theory of Bartschat and Grum-Grzhimailo [6] for the amplitude.

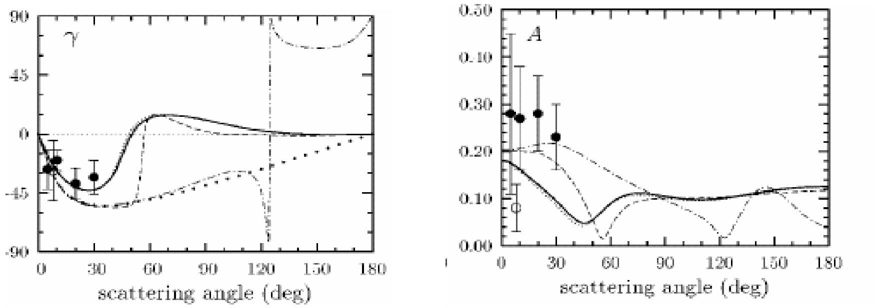

FIGURE 2. The amplitude A and alignment angle γ (deg) of correlations measured at an incident energy of 200 eV and a scattered electron energy of 133.4 eV, as a function of the scattered electron energy. Experiment: closed circles, Dogan *et al* [10], open circles, Hayes and Williams [12]. The various theoretical curves are from Bartschat and Grum-Grzhimailo [6].

(e,2e) Studies

Figure 3 shows (e,2e) data for the $He^+(n = 1, 2, 3, 4)$ states and e,(3 – 1)e data for He^{++} [11] at an incident energy of 200 eV, scattering angle of 11^o and a slow electron energy of 10 eV. A further disadvantage of the (e,2e) method is that it cannot isolate individual angular momentum states for each *n* value in helium. The *n* = 1 data show the expected shape under these kinematics, with a large binary peak close to the momentum transfer direction **K**, and a small recoil signal, in agreement with earlier data [15]. The higher *n* states show very different behaviours. All have more complex binary and recoil signals of similar size and without well defined peaks in the **K** and **–K** directions, respectively. This almost certainly reflects the different contributions of the increasing number of angular momentum states with increasing *n*.

The e,(3 – 1)e data were the first reported in which the correlation between a fast (scattered) and a slow electron were observed. A similar lack of symmetry about **K** is seen for the He^{++} data as for the excited He^+ states.

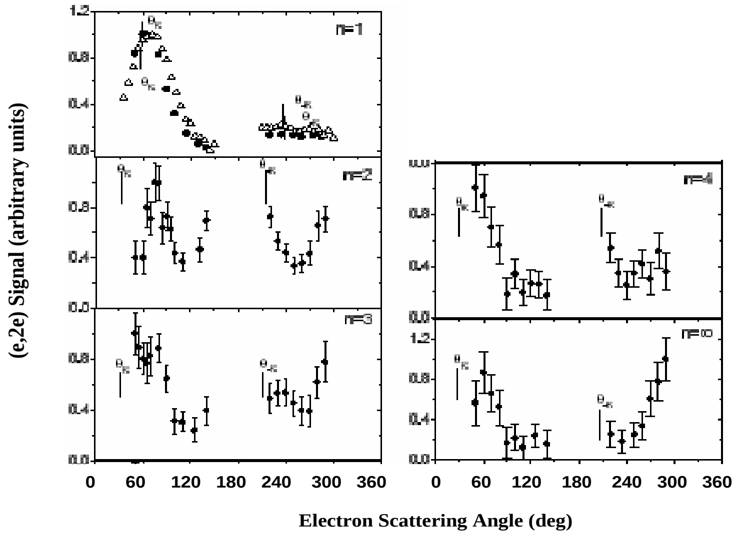

FIGURE 3. (e,2e) data for the He^+ (n = 1, 2, 3, 4) states and e, (3 - 1)e data for He^{++} (labeled $n = \infty$). The incident energy is 200 eV, the scattering angle 11^o and the ejected energy 10 eV. The data are from Dogan and Crowe [11]. For n = 1, comparison is made with the data of Schlemmer et al [15] at 250 eV and 12^o. For each n the vertical lines at forward angles show the direction of momentum transfer, θ_K, and at backward directions, θ_{-K}.

CALCIUM

The process,

$$e + Ca\,(4s^2)\,{}^1S \rightarrow Ca^+\,(4p)\,{}^2P_{3/2} + e\,(\text{scattered}) + e\,(\text{ejected})$$
$$\downarrow$$
$$Ca^+\,(4s)\,{}^2S_{1/2} + h\nu\ (393.3\ \text{nm}),$$

has been studied using the (e,eγ) technique. Care has been taken to isolate the $^2P_{3/2}$ ion state from the isotropic $^2P_{1/2}$ state.

Figure 4 shows the DDCS as a function of the detected (fast scattered) electron energy for the $Ca^+(4p)$ $^2P_{3/2}$ state at an incident electron energy of 400 eV. The electron scattering angle is 5^o and the photons are detected perpendicular to the scattering plane. The DDCS has the expected maximum at a threshold energy of 9.25 eV (zero ejected electron energy), followed by a decrease as the detected electron energy decreases. In this case the structures around 2.5 – 5 eV above the threshold can be associated with population of the $4^2P_{3/2}$ state by cascade from higher-lying ion states. The other pronounced sharp feature is the near-zero DDCS at an ejected energy around 8.2 eV.

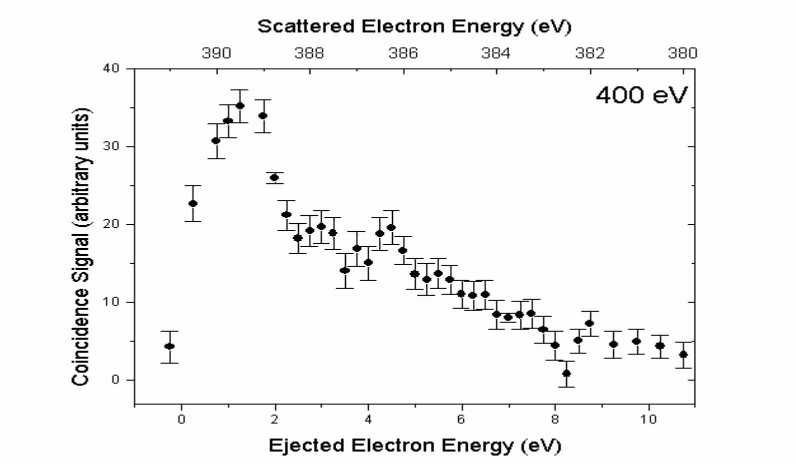

FIGURE 4. DDCS for Ca^+ (4p) $^2P_{3/2}$ at an incident energy of 400 eV and near-maximum scattered electron energies.

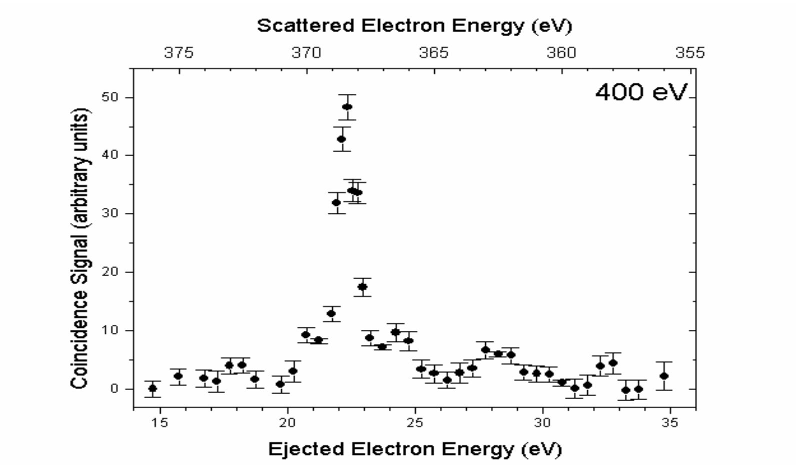

FIGURE 5. DDCS for Ca^+ (4p) $^2P_{3/2}$ at an incident energy of 400 eV and ejected electron energies close to the GDR energy. Note that the vertical scale is the same as in figure 4.

A major feature of the DDCS is the very large peak at a detected (scattered) electron energy of 368.6 eV, figure 5. This is due to autoionization of the $3p^5 4s^2 3d\ ^1P_1$ state of calcium (the giant dipole resonance, GDR) to Ca^+ (4p) $^2P_{3/2}$. The size of this peak in the DDCS due to this indirect process illustrates the importance of the promotion of a

3p electron to the empty 3d shell in calcium. It is also clear from the various smaller other neutral states of different configurations and symmetries contribute to the observed DDCS. For example, the structure at a detected electron energy of ~ 363 eV can be associated with doubly excited $3p^5 3d4s nl$ states. The only previous electron impact studies of the GDR and other states in this energy region have observed the electron emission from these states [16].

ACKNOWLEDGMENTS

This work is supported by the United Kingdom Engineering and Physical Sciences Research Council (EPSRC).

REFERENCES

1. Eminyan, M., MacAdam, K.B., Slevin, J. and Kleinpoppen, H., *Phys. Rev. Lett.* **31**, 576-9 (1973).
2. Bray, I. and Stelbovics, A. T., *Phys. Rev. A* **46**, 6995-7011 (1992).
3. Bartschat, K., Hudson, E. T., Scott, M. P., Burke, P.G. and Burke, V. M., *J. Phys. B: At. Mol. Opt. Phys.* **29**, 115-23 (1996).
4. Lahmam-Bennani, A., *J. Phys. B: At. Mol. Opt. Phys.* **24**, 2401-42 (1991).
5. Balashov, V. V. and Bodrenko, I. V., *J. Phys. B: At. Mol. Opt. Phys.* **32**, L687-92 (1999).
6. Bartschat, K. and Grum-Grzhimailo, A. N., *J. Phys. B: At. Mol. Opt. Phys.* **35**, 5035-50 (1999).
7. Dogan, M., Lohmann, B., Cvejanovic, D. and Crowe, A., in *XXII-ICPEAC Abstracts*, edited by S. Datz et al., Rinton Press, New Jersey, 2001, p. 181.
8. Hamdy, H., Beyer, H-J. and Kleinpoppen, H., *J. Phys. B: At. Mol. Opt. Phys.* **23**, 1671-7 (1990).
9. Bartschat, K. and Fang, Y., in *Correlations, Polarization, and Ionization in Atomic Systems*, edited by D. H. Madison and M. Schulz, AIP Conference Proceedings 604, Melville, New York, 2001, pp. 202 - 9.
10. Dogan, M., Crowe, A., Bartschat, K. and Marchalant, P. J., *J. Phys. B: At. Mol. Opt. Phys.* **31**, 1611-24 (1998).
11. Dogan, M. and Crowe, A., *J. Phys. B: At. Mol. Opt. Phys.* **33**, L461-5 (2000).
12. Hayes, P. A. and Williams, J.F., *Phys. Rev. Lett.***77**, 3098-101 (1996).
13. Dogan, M. and Crowe, A., *J. Phys. B: At. Mol. Opt. Phys.* **35**, 2773-81 (2002).
14. Balashov, V. V., in *The Physics of Electronic and Atomic Collisions*, edited by Y. Itikawa et al., AIP Conference Proceedings 500, Melville, New York, 2000, pp. 319 - 28.
15. Schlemmer, P., Srivastava, M. K., Rosel, T. and Ehrhardt, H., *J. Phys. B: At. Mol. Opt. Phys.* **24**, 2719-36 (1991).
16. Feuerstein, B., Zatsarinny, O. I. and Mehlhorn, W., *J. Phys. B: At. Mol. Opt. Phys.* **33**, 1237-54 (2002).